Food Chemistry: X 21 (2024) 101177

Contents lists available at ScienceDirect

Food Chemistry: X

journal homepage: www.sciencedirect.com/journal/food-chemistry-x

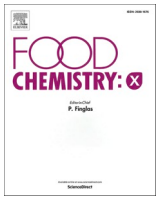

High hydrostatic pressure induced gastrointestinal digestion behaviors of quercetin-loaded casein delivery systems under different calcium concentration

Minjie Liao [1], Wei Li [1], Lu Peng, Jiahao Li, Jinbo Ren, Kaixin Li, Fang Chen, Xiaosong Hu, Xiaojun Liao, Lingjun Ma, Junfu Ji [*]

College of Food Science and Nutritional Engineering, National Engineering Research Center for Fruit and Vegetable Processing, China Agricultural University, Key Lab of Fruit and Vegetable Processing, Ministry of Agriculture and Rural Affairs, Beijing 100083, China

ARTICLE INFO

Keywords:
Casein micelle
HHP
Exogenous calcium
In vitro digestion
Digestive behavior

ABSTRACT

Casein micelle has a structure of outer hydrophilicity and inner hydrophobicity, its typical digestion characteristic is gastric coagulation. Based on calcium content as the key factor to control this process, high hydrostatic pressure (HHP) was firstly used to modify the micelle structure by mediating the tight connection between casein molecules themselves and with colloidal calcium, then the quercetin-loaded delivery systems were prepared. And in order to investigate the effect of exogenous calcium, calcium chloride was added for digestion. The results indicated that HHP broke the limitation of casein micelles as delivery carriers for hydrophobic components and increased the EE from 51.18 ± 3.07 % to 76.17 ± 3.41 %. During gastric digestion, higher pressure and exogenous calcium synergistically increased the clotting ability and inhibited the release of quercetin. In the small intestine, curds decomposed more slowly under higher pressure and calcium concentration, so the degradation of quercetin was effectively inhibited.

1. Introduction

As a major dietary source in daily life, bovine milk's main function is to supplement the human body with nutrients, especially protein. In bovine milk, there is about 32 g/L protein, of which 80 % is casein and 20 % is whey proteins (Farrell et al., 2004). Compared with whey protein, thousands of individual casein molecules including α-, β- and κ-casein typically aggregate into colloidal particles (hereinafter abbreviated as casein micelle) under the interaction of colloidal calcium phosphate (CCP) and non-covalent interactions (Broyard & Gaucheron, 2015). And among several types of molecular entities, both α- and β-casein are highly electronegative due to more phosphorylated serine residues, which makes them have stronger binding ability with calcium ion (Ca^{2+}). Therefore, the hydrophobic α- and β-casein are usually distributed within the micelles under calcium-mediated connection and hydrophobic interaction. But for hydrophilic κ-casein, which mainly interacts with other caseins and is located on the surface of micelles. It provides strong steric hindrance and repulsive force to hinder the aggregation between micelles, and ultimately determines the size of micelles (Huppertz, Heck, Bijl, Poulsen, & Larsen, 2021). All in all, this unique micelle structure endows casein with a wide range of processing properties. By controlling processing conditions (e.g. pH, salt, pressure, and temperature) (Fanny et al., 2017; Silva, Piot, De Carvalho, Violleau, Fameau, & Gaucheron, 2013), it is believed that the micelle structure of casein can be adjusted to meet different functional requirement.

High hydrostatic pressure (HHP) is a non-thermal processing technology, which is often applied to protein and can change protein structure by breaking relatively weak non-covalent interactions (Cepero-Betancourt, Opazo-Navarrete, Janssen, Tabilo-Munizaga, & Pérez-Won, 2020). In terms of the casein application, some studies have indicated that the structure of casein micelles is destroyed during the pressure build-up phase and holding time. According to reports, this pressure-induced casein micelle dissociation is caused by a weakening of hydrophobic and electrostatic interactions between casein molecules themselves and with colloidal calcium in CCP (Menéndez-Aguirre, Kessler, Stuetz, Grune, Weiss, & Hinrichs, 2014). With the release of pressure, these non-covalent interactions can be reactivated and induce different structural rearrangements. Quercetin is a hydrophobic

* Corresponding author.
E-mail address: junfu.ji@cau.edu.cn (J. Ji).
[1] Minjie Liao and Wei Li contributed equally to this work

https://doi.org/10.1016/j.fochx.2024.101177
Received 8 August 2023; Received in revised form 17 January 2024; Accepted 1 February 2024
Available online 6 February 2024

flavonoid commonly found in plants and vegetables, which has anti-inflammatory, antioxidant, antibacterial and other biological effects (Li et al., 2023). However, the development and utilization of quercetin are limited by its poor water solubility, instability, and low bioavailability (Li et al., 2019). As a suitable polyphenol delivery system, micellar casein-based delivery systems including nanoparticles and emulsions have showed great potential to solve these problems without compromising the biological activity of quercetin (Elzoghby, Helmy, Samy, & Elgindy, 2013; Ghasemi & Abbasi, 2014). Nevertheless, since the hydrophobic regions mainly located inside the micelles, natural casein micelles have poor loading capacity for hydrophobic substances. Under the action of HHP, the hydrophobic regions inside the micelles are expected to be exposed, making the rearranged micelle structure a more optimized carrier for quercetin.

In the gastrointestinal tract, the typical digestive characteristic of micellar casein-contained systems is coagulation in the stomach. In this process, the surface κ-casein hair layer of the micelles will be removed under the effect of low pH and pepsin. Subsequently, these exposed casein molecules will interact with each other and with Ca^{2+} in digestive fluid, which further leads to the cross-linking between particles and the formation of curds (Mcsweeney & Fox, 2013; Zhang et al., 2023). Based on previous studies, calcium content is considered as the key variable to control this digestion process. Specifically, it has been reported that removing 42 % of colloidal calcium through ion exchange weakened the coagulation level and accelerated the digestion of micellar casein (Wang, Ye, Lin, Han, & Singh, 2018). In addition, it was also found that gastric coagula of bovine casein micelles became looser with increasing decalcification level, especially up to 40 % under the infant conditions and up to 69 % under the adult and elderly conditions (Wang et al., 2023). And in the case of 13–63 % decalcification, there were no visible clusters and the degradation rate of bovine casein micelles was faster (Huppertz & Lambers, 2020). Overall, the purpose of calcium regulation in these studies is more focused on modifying the original micelle structure before digestion. While in the digestive tract, the introduction of exogenous calcium from complex food matrices may also have a great impact on the digestive behaviors of micellar casein-contained systems, which deserves more detailed exploration.

Therefore, the purpose of our study is to evaluate the effect of exogenous calcium introduced from food matrix on the digestive behaviors of recombinant micellar casein delivery systems. Based on that, the recombined casein micelles were first prepared at 100, 300 and 500 MPa, which were then used to load quercetin in the form of O/W emulsions. After characterizing the particle size, zeta potential, free calcium content and encapsulation efficiency (EE) of quercetin-loaded emulsions, the interaction forces of the system were evaluated through fluorescence spectrum and particle size changes after adding chemical blockers. Subsequently, an *in vitro* static digestion mode was used to explore the digestion behaviors of the emulsions after spray drying, including the dynamic quercetin release, solubility, particle size and proteolysis. More importantly, considering the complexity of food matrices, calcium chloride was added before digestion to simulate the effect of exogenous calcium on the digestive behaviors of the delivery systems. Compared with the previous results, this research will make further progress in developing new micellar casein-based delivery systems, and further elucidate their interactions with other food components during digestion.

2. Materials and methods

2.1. Materials

Analytical quercetin standard with a purity greater than 98 % was obtained from Shanghai Yuanye Bio-Technology Co., Ltd (Shanghai, China). Micellar casein powder with 86.98 % protein content came from Wapakoneta Ingredia Co., Ltd (Wapakoneta, America). Soybean oil and anhydrous ethanol were purchased from Macklin Biochemical Technology Co., Ltd (Shanghai, China). Digestive enzymes including porcine Pepsin (P7012) and porcine Pancreatin (P7545) were purchased from Sigma-Aldrich Trading Co., Ltd (St. Louis, MO, USA). The Ca^{2+} standard solution and strength regulator were purchased from Mettler Toledo International Trade Co., Ltd (Zurich, Switzerland). Other chemical reagents such as bile salt, anhydrous calcium chloride, sodium chloride (NaCl), sodium dodecyl sulfate (SDS) and urea were obtained from Solarbio Biotechnology Co., Ltd (Beijing, China).

2.2. Preparation of quercetin-loaded O/W emulsions

Briefly, powdered micellar casein was resuspended in deionized water with a concentration of 7 % (*w/w*), and stirred at room temperature at a speed of 700 rpm for 12 h. The formed suspension was then centrifuged (3000 *g*, 10 min) to obtain the casein supernatants. After being packaged into polyethylene bags and sealed, these casein supernatants were subjected to HHP treatment at the pressure of 0, 100, 300 and 500 MPa, respectively, for 10 min. In subsequent experiments, they were named CN, CN100, CN300, and CN500, respectively. The oil phase solution was prepared by adding the quercetin standard into soybean oil with a ratio of 0.08 % (*w/w*) through magnetic stirring for 20 min. In order to prepare O/W emulsion, previously prepared CN, CN100, CN300 and CN500 protein solution was mixed with the oil phase solution at a ratio of 9:1 (*v/v*), respectively. After being stirred evenly and sheared at a speed of 10000 rpm for 5 min, the mixtures were homogenized with a high-pressure homogenizer (JN-10HC, Guangzhou Juneng Nano&Bio Technology Ltd., Guangzhou, China) at 600 bars for three times to obtain quercetin-loaded O/W emulsions. Immediately, the basic physicochemical properties of these prepared emulsions were characterized. And based on previous parameters (Liao, Ma, Miao, Hu, & Ji, 2021), these emulsions were quickly spray dried with a mini spray-dryer (B-290, Büchi Corporation, Flawil, Switzerland) to obtain dry powder samples, which were named CQ, CQ100, CQ300 and CQ500 in turn.

2.3. The physicochemical properties of O/W emulsions

2.3.1. The particle size, PDI, zeta potential and visible appearance characterization

In this part, the particle size, PDI, and zeta potential of CQ, CQ100, CQ300 and CQ500 O/W emulsions were characterized by a Zetasizer (Zetasizer ZEN 3700, Malvern Instruments Ltd., Worcestershire, UK) at 25 ℃ and their visible appearance was recorded through photography. Before adding the samples to the measurement cell of Zetasizer, each sample was diluted 200 times with deionized water and thoroughly mixed to avoid interference from multiple scattering. During the measurement, the equilibrium time was set to 120 s, and each sample was measured three times in parallel.

2.3.2. Determination of free calcium content of O/W emulsions

Here, the Ca^{2+} analyzer (S220, Mettler Toledo International Trade Co., Ltd, Flawil, Switzerland) was used to measure the free Ca^{2+} concentration of several O/W emulsions. Before measurement, it was necessary to calibrate the Ca^{2+} selective electrode by using the standard solutions containing 10, 100 and 1000 mg/L Ca^{2+}, respectively. After that, all samples were mixed with Ca^{2+} strength regulator at a ratio of 50:1 (*v/v*) for measurement.

2.3.3. Determination of EE of O/W emulsions

Based on previous study (Tan et al., 2014) and with some modifications, the EE of O/W emulsions was measured. Before the measurement, the O/W emulsions were centrifuged at 10000 rpm for 20 min to separate unencapsulated quercetin crystals (W_1), and mixed with absolute ethanol to determine the absorbance at 373 nm. In addition, the content of quercetin used to prepare emulsions was considered as the total quercetin content (W). The content of quercetin was calculated through the standard curve, which was achieved by dissolving the

quercetin standard in absolute ethanol to reach the concentration of 4, 6, 8, 12, 16, 20 μg/mL. Therefore, the EE of quercetin could be calculated using the Eq. (1):

$$\text{EE}\ (\%) = \frac{\text{W-W1}}{\text{W}} \times 100\% \quad (1)$$

2.4. Determination of the interactions

2.4.1. The effect of NaCl, SDS, and urea on the interactions

In order to verify the main types of interaction forces in the system, blocking agents such as NaCl (500 mM), SDS (0.8 %, w/v), and urea (4.8 M) were added into the rehydrated microparticle solutions to destroy electrostatic interactions, hydrophobic interactions, and hydrogen bonds (Li & Zhong, 2020). Specifically, the dominant interaction force was judged by the particle size changes before and after the addition of these blocking agents. And it was worth noting that the solvents used for microparticle rehydration and dilution needed to be replaced with the corresponding blocking agent solutions.

2.4.2. Fluorescence spectroscopy

In the pre-processing, the spray-dried microparticles (CQ, CQ100, CQ300 and CQ500) and corresponding proteins (CN, CN100, CN300 and CN500) treated under different pressure conditions were rehydrated in phosphate buffer at a concentration of 0.4 mg/mL. Subsequently, their fluorescence intensity curves in the range of 300–400 nm were recorded by a spectrofluorometer (FS5, Edinburgh Instruments, Scotland, UK) at the excitation wavelength of 280 nm. During data processing, the fluorescence intensity of the phosphate buffer background was subtracted from that of the samples.

2.5. In vitro static digestion

In this part, the final protocol of *in vitro* static digestion was based on the previous study (Brodkorb et al., 2019) and made some modifications. First, the gastric and intestinal electrolyte solutions were prepared in advance, and their pH was adjusted to 3 and 7, respectively. During gastric digestion, Pepsin was added to achieve an enzyme activity of 2000 U/mL. During the intestinal digestion, both Pancreatin and Bile salt were added to achieve an enzyme activity of 100 U/mL and a salt concentration of 10 mM. During 2 h gastric and intestinal digestion period, a water bath constant temperature oscillator (SHZ-C, Shanghai Boxun Co., Ltd, Shangha, China) was selected to ensure constant oscillation speed (120 rpm) and temperature (37 ℃). In order to explore the impact of exogenous calcium as a nutritional supplement in food, solid calcium chloride was thoroughly mixed with CQ, CQ100, CQ300 and CQ500 powder before digestion. And based on 0.15 mM Ca^{2+} concentration in the original gastric electrolyte, different amounts of calcium chloride were added to ensure the Ca^{2+} concentration of 0.15, 2 and 5 mM in the stomach. At the beginning of digestion, powder samples were added to gastric electrolyte solutions and stirred for 30 s to simulate powders wetting before consuming. At the end of stomach digestion, the pH of the mixture was immediately adjusted to 7.0 to inactivate Pepsin. Later, the intestinal electrolyte solutions were added to gastric chyme at the ratio of 1:1 (*v/v*) to carry out continuous intestinal digestion. At several fixed times, a certain volume of digestive mixture was collected to characterize the release of quercetin, solubility change, particle size change and protein hydrolysis degree.

2.5.1. The release of quercetin during in vitro digestion

Based on previous method (Liu et al., 2020), the release ratio of quercetin was measured at 5, 30, 60, 90, 120, 125, 150, 180, 210, 240 min, respectively, during *in vitro* digestion. In detail, 3 mL of digested mixtures were removed and centrifuged at 10000 rpm for 20 min to obtain the micelle layers. After mixing with anhydrous ethanol, the absorbance value at 373 nm was measured to obtain the released quercetin content during digestion (W_1). Before digestion, a certain amount of powder was fully mixed with anhydrous ethanol and centrifuged. Later, the total quercetin content (W) was obtained by measuring the absorbance value at 373 nm. Therefore, the release ratio of quercetin over time was calculated using the Equation (2):

$$\text{Cumulative release}\ (\%) = \frac{\text{W1}}{\text{W}} \times 100\% \quad (2)$$

2.5.2. Characterization of solubility and visible appearance during in vitro digestion

At 5, 30, 60, 90, 120, 125, 150, 180, 210, 240 min, the *in vitro* digestion process was terminated, and all digestion samples were taken from the water bath oscillator. After centrifugation at 3000 *g* for 10 min, the precipitates were collected and dried to constant weight (W_1) at 105 °C by an electric blast drying oven (XMTD-8222, Shanghai Jing Hong Laboratory Instrument Co., Ltd, Shanghai, China). Meanwhile, the dry weight of the samples before digestion (W) and blank digestion solution without sample addition was measured (W_0), which was further used to calculate solubility over time according to Equation (3). And in order to record the visible dissolution and aggregation during digestion, the remaining residues after simply filtering the supernatants were also placed in glass plates for real-time photography.

$$\text{Solubility}\ (\%) = \frac{\text{W} + \text{W0-W1}}{\text{W}} \times 100\% \quad (3)$$

2.5.3. Determination of particle size during in vitro digestion

At 5, 60, 120, 150 and 240 min during digestion, a laser particle size analyzer (LS 13320, Beckman Coulter Inc, Fullerton, CA, USA) was selected to track changes in particle size. In the case of configuring the PIDS-included liquid module, both small particles and large aggregates generated during digestion were effectively recorded under 55 % pump speed. During measurement, the collected digestion samples were not subjected to additional dilution, but directly added to the sample cell to achieve 8 % shading.

2.5.4. Determination of protein hydrolysis during in vitro digestion

During digestion, sodium dodecyl sulfate–polyacrylamide gel electrophoresis (SDS-PAGE) experiment was used to characterize the protein hydrolysis degree of delivery systems. At first, these digested mixtures collected at 5, 120, 125 and 240 min were heated in a boiling water bath for 5 min to inactivate the enzymes, and then freeze-dried into powder. Subsequently, the dried powder was redissolved in loading buffer to achieve the same protein concentration of 2 mg/mL. After boiling for 5 min and centrifuging at 10,000 *g* for 15 min, the supernatants were collected for electrophoresis. The electrophoresis gel used here was 4–20 % gradient gel, and the loading volumes of samples and marker were 10 and 5 μL, respectively. At the end of electrophoresis, Coomassie brilliant blue fast staining solution was used to dye the electrophoresis gel. And after decolorization by deionized water, the electrophoresis results were recorded by a gel electrophoresis imager (JY04S-3C, Beijing Jun Yi Electrophoresis Co., Ltd, Beijing, China).

2.6. Statistical analysis

In this study, all measurement indicators were subjected to three independent repeated experiments and expressed in the form of "mean ± standard deviation". The level of significant differences between different groups was judged by a software SPSS (version 24.0) at a significance level of $p = 0.05$.

3. Results and discussion

3.1. The physicochemical properties of quercetin-loaded O/W emulsions

As depicted in Fig. 1C, the free calcium content in soluble phase was

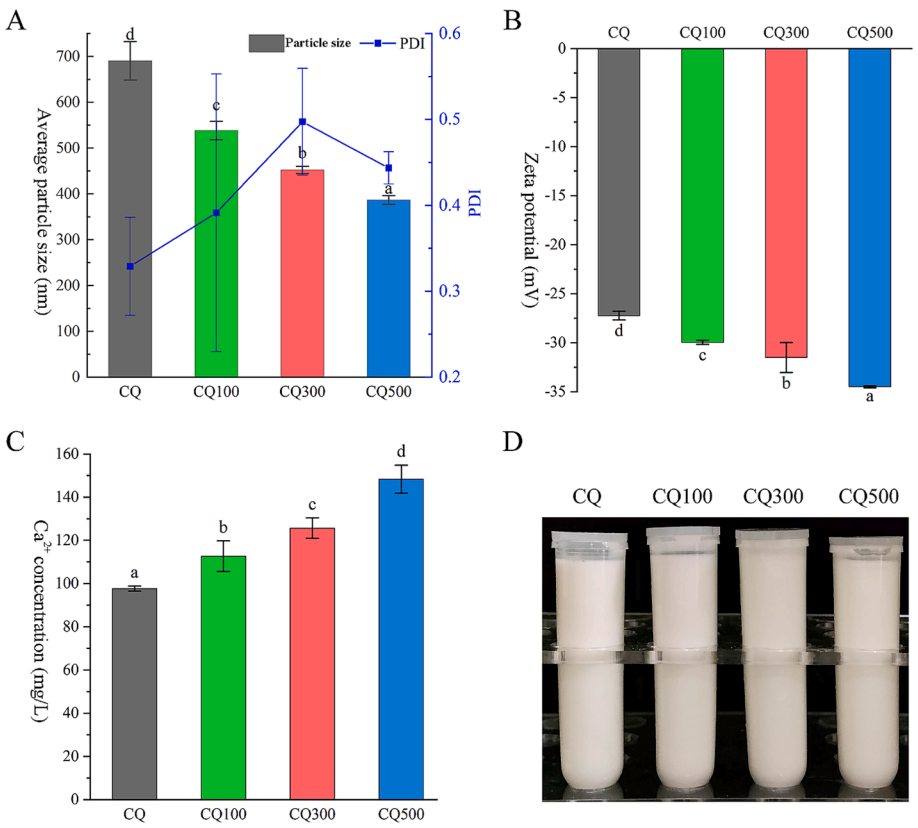

Fig. 1. The physicochemical properties of quercetin-loaded casein delivery systems. A: The particle size and PDI of delivery systems; B: The zeta potential of delivery systems; C: The free calcium content of delivery systems; D: The visible appearance of delivery systems.

increased from approximately 100 mg/L to approximately 150 mg/L under the action of HHP treatment. This result indicated that HHP treatment disrupted the CCP bridge, resulting in more free calcium being released into the soluble phase. With the loss of CCP, it was clear that the average particle size of the corresponding O/W emulsions in Fig. 1A was decreased from about 700 nm to about 400 nm with the increase of pressure. This result was consistent with previous studies, indicating that HHP could dissociate the original casein micelles and induce the generation of reformed casein micelles with smaller particle sizes (Iturmendi, García, Galarza, Barba, Fernández, & Maté, 2020). On the other hand, the generation of more fragments and reassemble units increased the heterogeneity of the system, so it could be observed in Fig. 1A that HHP treatment increased the PDI values of CQ100, CQ300, and CQ500 to varying degrees, with CQ300 having the highest PDI value. Looking at the zeta potential in Fig. 1B, the absolute value of surface charges increased from 14.93 ± 0.79 mV to 28.30 ± 1.30 mV, displaying higher electrostatic repulsion to prevent particle aggregation. According to the Holt model, CCP is formed by the interaction between phosphorylated serine and Ca^{2+} in casein micelles (Little & Holt, 2004). After breaking the CCP and releasing bound calcium, these negatively charged phosphorylated serine residues will be exposed, resulting in an increased surface negative charge. Focusing on the results in Fig. 1D, the visible appearance of O/W emulsions presented a uniform milky white without stratification, indicating good stability of these emulsions. Combined with the influence of HHP on the structure of casein micelles and corresponding emulsions, it could be said that the basic physicochemical properties of emulsions were mainly affected by the recombinant micellar structure. In general, natural casein micelles are formed under the interactions between individual casein molecules and the linkage of CCP. Under the influence of HHP, these interactions would be disrupted, and further leading to the formation of smaller reassociated micelles. After preparing the corresponding emulsions, these reassociated casein micelles were conducive to improve the stability of emulsions by providing stronger surface repulsion force.

3.2. The EE of quercetin-loaded O/W emulsions

Before spray drying, the EE of CQ, CQ100, CQ300, and CQ500 emulsions was measured, and the corresponding results were displayed in Fig. 2A. With the increase of pressure, it was obvious that the EE of quercetin-loaded emulsions gradually increased from 51.18 ± 3.07 % to 76.17 ± 3.41 %, exhibiting superior emulsification ability of recombinant casein micelles. Natural casein micelle has a natural self-assembled structure with hydrophilic outer layer and hydrophobic inner core. Under the action of HHP, this natural structure will be destroyed into micelle fragments in the presence of pressure and further reorganized when pressure is released. And the reorganized casein micelles are usually not in the same organizational state as before the pressure treatment. Based on previous studies, HHP could increase the surface hydrophobicity by exposing more internal hydrophobic molecules (Mao, Ni, Ma, Chen, Hu, & Ji, 2022). Therefore, these reorganized casein micelles were easier to adsorb at the interface of oil globules and participate in the emulsification process (Nassar et al., 2021). From another perspective, protein emulsifiers with smaller particles size and higher dispersibility were also conducive to the formation of finer and more stable emulsions (Meena, Singh, Arora, Borad, Sharma, & Gupta, 2017), so more quercetin could be better retained in the oil phase.

3.3. The interactions of the delivery systems

3.3.1. The effect of NaCl, SDS, and urea on the interactions

As shown in Fig. 2B, the particle sizes of microparticles before and after adding NaCl, SDS and Urea were compared. When it came to CQ, their original particle size was about 700 nm, which was significantly

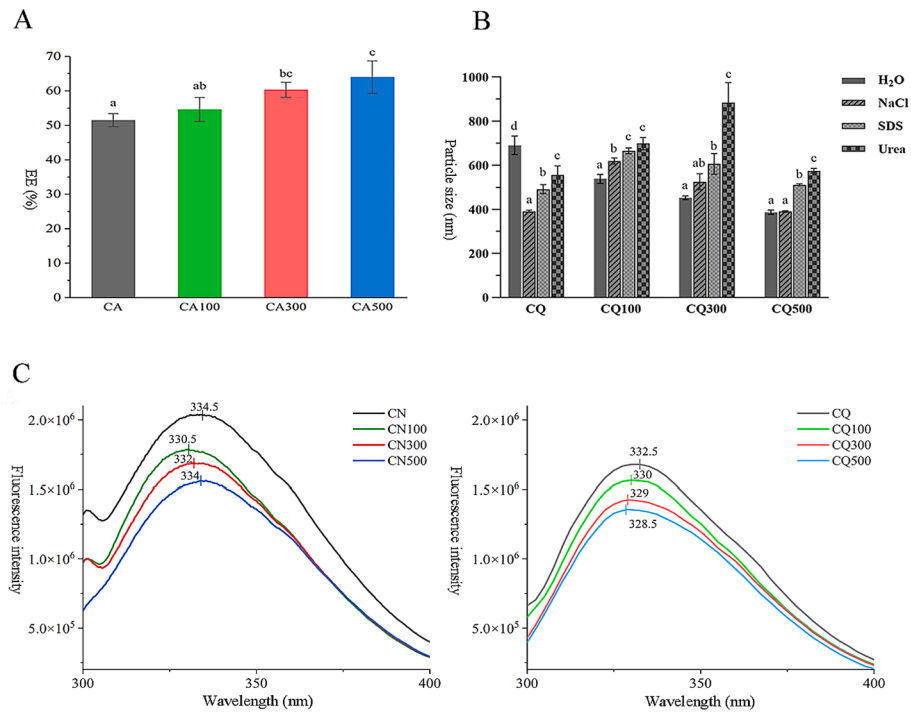

Fig. 2. The EE and interactions of quercetin-loaded casein delivery systems. A: The EE of delivery systems; B: The effects of NaCl, SDS and urea on the interactions of delivery systems; C: The fluorescence spectrum results of delivery systems.

reduced after adding three blocking agents. Among them, it was evident that the addition of NaCl and SDS resulted in a greater reduction in particle size. This result suggested that electrostatic and hydrophobic interactions played a crucial role in maintaining the stability of the CQ system. While for samples treated with HHP, due to their smaller initial particle size, the addition of three blocking agents instead increased the particle size to varying degrees. And compared to the changes caused by NaCl, the degree of significant difference demonstrated that urea and SDS caused greater disturbance to these systems. Therefore, it could be concluded that the main forces responsible for stabilizing CQ100, CQ300, and CQ500 systems were hydrogen bonds and hydrophobic interactions. And by analyzing the differences in the interaction forces before and after HHP, it could be inferred that HHP mainly destroyed electrostatic forces compared to the other two forces.

In casein micelles, it is well known that α-, β- and κ-casein are held together by non-covalent interactions, especially the hydrophobic interaction between proteins and the electrostatic interaction between phosphoserine and colloidal calcium. At lower EE, the binding force between quercetin-contained oil phase and casein micelles was weak in CQ system, so the molecular forces inside the casein wall materials dominated the whole system. During the pressure build-up and holding phase, both hydrophobic interaction and electrostatic interaction were disrupted (Menéndez-Aguirre, Kessler, Stuetz, Grune, Weiss, & Hinrichs, 2014). And as discussed in Section 3.1, colloidal calcium lost a lot during this process. Therefore, it could be inferred that the reversibility of electrostatic interactions during pressure release was much lower than that of hydrophobic interactions. In other words, HHP caused more severe irreversible damage to electrostatic forces. As pressure increased, these recombinant casein micelles were more likely to bind the quercetin-contained oil phase through hydrophobic interaction and hydrogen bond (Bourassa, Bariyanga, & Tajmir-Riahi, 2013; Hudson, Rezende, Campos de Paula, Coelho, Mendes da Silva, & dos Santos Pires, 2019). Therefore, it could be seen that the main interaction forces underwent a significant transformation after HHP treatment.

3.3.2. *Fluorescence spectroscopy*

As depicted in Fig. 2C, the fluorescence intensity of individual proteins was always higher than that of corresponding delivery systems. By comparing the value of λ_{max}, there was an obvious blue shift phenomenon after loading quercetin. Combining the above results, it could be inferred that quercetin has successfully combined with casein. When it came to the changes caused by HHP treatment, varying degrees of blue shift could be easily found. And further focusing on the impact of pressure levels, it was evident that the increase in processing pressure led to a continuous decrease in fluorescence intensity.

In general, λ_{max} excited at 280 nm is mainly used to characterize the microenvironment of tryptophan residues, because phenylalanine has a very low quantum yield and the fluorescence of tyrosine is almost quenched in most cases. In casein micelles, there are five tryptophan residues, which are mainly distributed in the internal hydrophobic core of casein molecules. In addition, the shift of λ_{max} usually represents the changes in local environment where these endogenous tryptophan residues are located. Therefore, the changes in fluorescence spectra can provide important information about the self-assembly of casein molecules and the impact of ligand binding. Under the effect of HHP, casein micelles were firstly decomposed and then reconstituted. Consequently, the fluorescence quenching and blue shift corresponded well to the conformational change of casein micelles (Han, Wang, Wang, & Tang, 2020). After binding quercetin, the hydrophobic portion of recombinant micellar casein would be occupied, reducing the number of tryptophan groups exposed to the water environment (Ke et al., 2023). And based on the results in Section 3.2, these endogenous hydrophobic amino acids were easier to bind to quercetin-contained oil phase under higher pressure. Therefore, the degree of fluorescence quenching and blue shift increased with increasing pressure.

3.4. *The dynamic release of quercetin during in vitro digestion*

During *in vitro* simulated digestion, the release of quercetin from CQ, CQ100, CQ300 and CQ500 microparticles at 0.15, 2, and 5 mM Ca^{2+} was shown in Fig. 3A. In the stomach, it was obvious that the release content

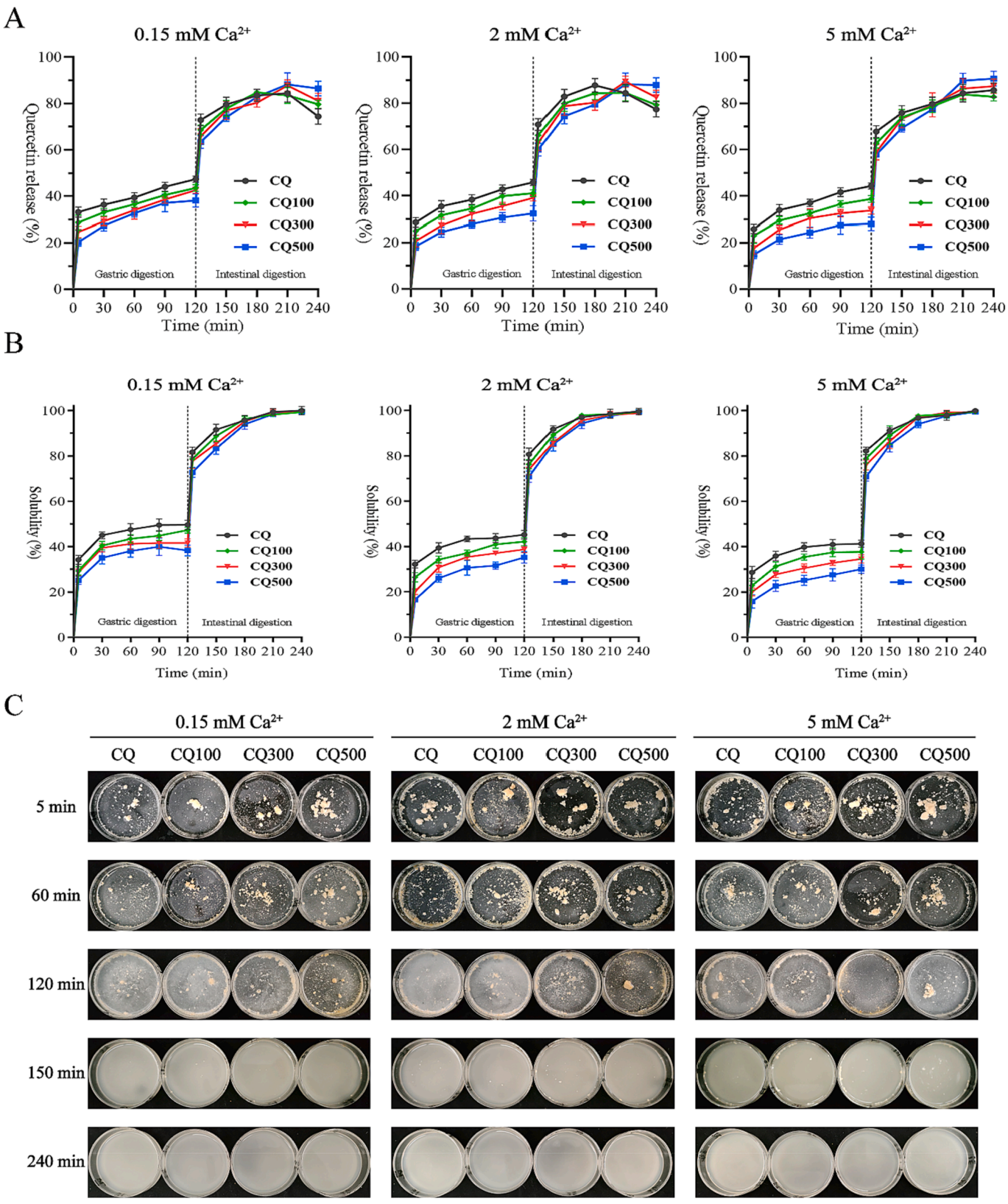

Fig. 3. The quercetin release and solubility of quercetin-loaded casein delivery systems during *in vitro* digestion. A: The dynamic release of quercetin during *in vitro* digestion; B: The solubility of delivery systems during *in vitro* digestion; C: The visible appearance of delivery systems during *in vitro* digestion.

of quercetin increased rapidly within 5 min. And the higher the pressure, the lower the quercetin release at this point. Later, the gastric release of quercetin always kept rising with digestion time. In the small intestine, the release of quercetin increased in the early stage, but began to show a slight downward trend in the middle and later stages of digestion. Focusing on the impact of HHP, the increased pressure continuously reduced the release of quercetin in the stomach. When the pressure increased from 0 to 500 MPa, it could be easily observed that the corresponding gastric release content decreased by 9 %, 13 %, and 16 % at 0.15, 2, and 5 mM Ca^{2+}, respectively. This trend basically lasted until the first 30 min of intestinal digestion, but gradually reversed afterwards. At the end of intestinal digestion, it seemed that the higher the pressure, the higher the release of quercetin. On the other hand, it was interesting that the increase of Ca^{2+} reduced the release of quercetin in the stomach under fixed pressure. When the concentration of Ca^{2+} increased from 0.15 mM to 5 mM, the gastric release ratio of CQ, CQ100, CQ300 and CQ500 microparticles decreased by 3 %, 4.8 %, 8.8 % and 9.9 %, respectively. In the intestinal digestion stage, this trend induced by Ca^{2+} only lasted for 5 min. In the subsequent stage, Ca^{2+} instead played an important role in delaying the degradation of quercetin. At 0.15 and 2 mM Ca^{2+}, the released quercetin started to degrade in large quantities about 180 min in the intestine. But after adding 5 mM Ca^{2+}, the release of quercetin decreased slightly after 210 min. Basically, it could be said that the synergistic effect of Ca^{2+} and HHP reduced the release of quercetin in the stomach. Evidently, the gastric release of CQ500 at 5 mM Ca^{2+} was only 28.12 ± 3.02 %, but the gastric release rate of CQ release rate at 1.5 mM Ca^{2+} was as high as 47.31 ± 1.31 %. In the intestinal phase, the coexistence of higher pressure and more Ca^{2+} mainly reduced the degradation of quercetin by delaying the release of quercetin. As depicted in Fig. 3A, the degradation amount of CQ at 1.5 mM Ca^{2+} in the intestine was at least up to 10 %. While for CQ500 at 5 mM Ca^{2+}, there was no obvious degradation leading to the reduction of quercetin release.

During digestion, the release of quercetin was mainly affected by the micelle structure before digestion and the structural rearrangement of micelles during digestion. And these two factors could be effectively adjusted by HHP treatment and the addition of exogenous calcium. On the one hand, HHP effectively improved the physicochemical properties of delivery systems. Among them, the improvement of stability and EE was conducive to reducing the release of quercetin. Based on previous studies, the structural rearrangement of delivery systems induced by the coagulating of micellar casein could effectively inhibit the release of active substances (Sadiq, Gill, & Chandrapala, 2021; Ye, 2021). Before digestion, HHP modified the structure of casein micelles, and these casein micelles treated with higher pressure would expose more internal hydrophobic casein molecules, mainly for α- and β-casein. Compared with κ-casein, α- and β-casein have more phosphoserine for calcium binding (Boland, Golding, & Singh, 2014). After adding exogenous calcium, the available Ca^{2+} in the digestive fluid increased. Therefore, these recombined micelles would undergo a higher degree of structural rearrangement under the synergistic effect of higher pressure and calcium concentration, which would be verified in the following experiments. In this case, it was obvious that the release of quercetin would be reduced due to the stronger structural barrier. After entering the small intestine, the gastric structural rearrangement would not be supported by the intestinal environment. Without enough structural barriers, the embedded quercetin would escape quickly. The released quercetin was unstable under alkaline conditions and prone to degradation (Yin et al., 2022). When the degradation amount of quercetin was greater than the release amount, it could be observed that the release curve of quercetin showed a downward trend. Under higher pressure and Ca^{2+} concentration, it was speculated that the gastric rearrangement structure had stronger resistance and collapsed more slowly. Therefore, the degradation amount of quercetin in these samples was much lower at the end.

3.5. Changes in solubility and visible appearance during in vitro digestion

In Fig. 3B and C, the solubility and visible appearance results of the microparticles during *in vitro* digestion were shown, respectively. In the stomach, the solubility of microparticles was at most 49.67 ± 2.07 %, which was much lower than the solubility in the small intestine. By observing the results in Fig. 3C, it could be seen that many different sizes of curds were quickly formed at 5 min. These curds were continuously hydrolyzed over digestion time, and most of them have disappeared after 30 min of intestinal digestion. If focused on the influence of individual pressure or Ca^{2+}, it seemed that the impact of pressure was greater. When the pressure increased from 0 to 500 Mpa, the solubility decreased by 11.34 %, 10.05 %, and 11.25 % at three fixed Ca^{2+} concentrations. But when the Ca^{2+} concentration was variable, it could be seen that the solubility of CQ, CQ100, CQ300 and CQ500 microparticles decreased by about 8.35 %, 9.60 %, 7.00 %, and 8.26 %, respectively. When it came to the synergistic effect of pressure and Ca^{2+}, simultaneously increasing both resulted in more curds and tighter structures. At 0 MPa and 1.5 mM Ca^{2+}, there was still about 50 % of the insoluble part at the end of gastric digestion. While at 500 MPa and 5 mM Ca^{2+}, nearly 70 % of the microparticles remained undissolved in the end. This trend of solubility persisted until 180 min of intestinal digestion. At 210 min, almost all the microparticles have been completely dissolved.

During digestion, the solubility change of particles was mainly caused by the coagulating behaviors of casein, because the coagulating particles mainly contributed to these insoluble parts. And comparing the results of solubility and release, it was not difficult to find that the changing trends of the two indicators were basically consistent, indicating a close connection between the two. Based on the result in Section 3.2, there was still a part of quercetin on the surface of microparticles. Without wall material barriers, there was no doubt that these quercetin molecules would dissolve out in 5 min. The increased pressure contributed to the increase of EE, so it could be seen that the initial dissolution of quercetin decreased under higher pressure. Accompanied by the rapid dissolution of microparticles, the gastric environment immediately triggered the protein curdling. Generally, casein micelles are stabilized by steric hindrance and electrostatic effect provided by κ-casein. During gastric digestion, the acidic environments could lead to the collapse of κ-casein on the surface of micelles by neutralizing the net-negative charges of κ-casein (De kruif, 1999). On the other hand, the existence of Pepsin could cut off the C-terminal hair layer of κ-casein, leaving *para*-κ-casein on the surface of micelles. At this time, the remaining *para*-κ-casein micelles would interact with each other to induce coagulation (Huppertz & Chia, 2021). Under the effect of HHP, more exposed hydrophobic α- and β-casein molecules were expected to form cross-linked CCP calcium bridges under the induction of free calcium. And with the addition of exogenous calcium, the number of cross-linked CCP calcium bridges would also increase. Therefore, some larger and harder curds were formed under higher pressure and Ca^{2+} concentration, and they showed stronger ability to inhibit the release of quercetin. The structure of these curds became more looser over digestion time, leading to the constant escape of quercetin. And just as previous studies, alkaline pH and Pancreatin in the intestine caused rapid breakdown of gastric curds (Nguyen, Bhandari, Cichero, & Prakash, 2015), resulting in a large jump of release content after only 5 min of intestinal digestion. Wherein, these larger curds formed under higher pressure and Ca^{2+} concentration disintegrated more slowly and had a longer intestinal residence time. Therefore, these microparticles could continuously inhibit release and avoid the degradation of quercetin.

3.6. Changes in particle size during in vitro digestion

As shown in Fig. 4, the particle size of all microparticles was mainly distributed between 10 and 1000 nm in the stomach, and their average particle size had exceeded 150 nm at 5 min of gastric digestion. When pressure and Ca^{2+} concentration increased, it could be seen that the

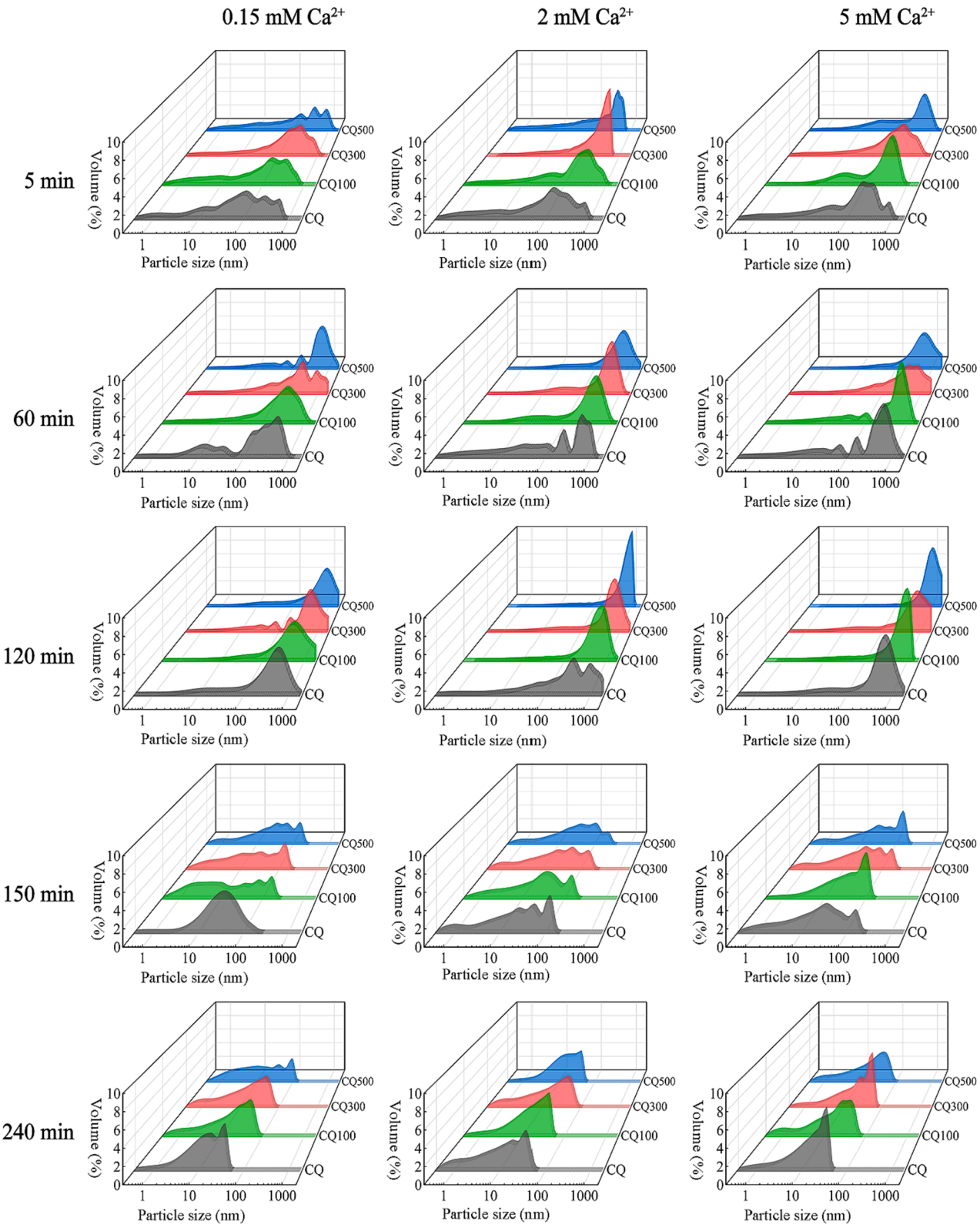

Fig. 4. The particle size changes of quercetin-loaded casein delivery systems during *in vitro* digestion.

particle size distribution further shifted to the range of 100–1000 nm. As time went by, the particles with an average diameter exceeding 500 nm gradually increased, and their particle size distribution also showed an increasing trend. Throughout the entire gastric digestion, it was clear that the influence of pressure and Ca^{2+} concentration on particle size distribution remained unchanged. At the end of gastric digestion, the average particle size of CQ samples under 1.5 mM Ca^{2+} was approximately 480 nm, while the average particle size of CQ500 samples under 5 mM Ca^{2+} was as high as about 1000 nm. After entering intestinal digestion, it was evident that the particle size distribution of most microparticles rapidly decreased to below 100 nm after only 30 min. At the end of digestion, there was no microparticles with average diameter

exceeding 30 nm.

The particle size distribution could reflect the overall structural changes of heterogeneous samples. In the stomach, the higher particle size distribution was mainly caused by the aggregation of particles and the generation of curds. Based on the particle size distribution at 5 min, it proved again that the gastric coagulation was a very fast process. And consistent with the results in Fig. 3B and C, these recombinant structures treated under higher pressure had the ability to form larger curds during gastric digestion, and more available exogenous calcium further increased the degree of coagulation. Therefore, a higher particle size distribution could always be observed under higher pressure and Ca^{2+} concentration. During the intestinal period, these large curds were further broken down into dispersed entities and further hydrolyzed over time. As a result, it could be seen that the particle size in the intestine was much lower than that in the stomach and continuously decreased over time.

3.7. Changes in proteolysis during in vitro digestion

During *in vitro* digestion, the protein hydrolysis of different microparticles was depicted in Fig. 5. In the stomach, it was evident that the protein bands of all samples were mainly distributed in three regions, including approximately 70 kDa, 25–40 kDa, and 10–20 kDa. These regions persisted during gastric digestion, but exhibited differences due to pressure levels and Ca^{2+} concentrations. In detail, as the pressure level and Ca^{2+} concentration increased, it could be observed that the protein bands at approximately 70 kDa deepened. Based on previous studies, the protein band in 70 kDa might represent the aggregates formed between the same or different casein subunits (Du et al., 2023). In the range of 25–40 kDa, it was reported that several casein subunits including α-, β- and κ-casein mainly existed in this region (Do, Williams, & Toomer, 2016). And it could be seen that higher pressure and Ca^{2+} concentration caused protein bands to shift towards regions with higher molecular weights, which might also be the result of random cross-linking between casein molecules. Looking at the range of 10–20 kDa, two prominent protein bands near 10 kDa and 15 kDa could be observed in all samples, and it was difficult to identify the difference in band depth between samples. Among them, the protein band near 15 kDa might represent the *para*-κ-casein produced by κ-casein hydrolysis, and protein band of 10 kDa might also be derived from protein degradation (Trujillo, Guamis, & Carretero, 1998). After entering the intestine, all protein bands were distributed below 45 kDa, and they mainly represented peptides produced by trypsin hydrolysis. However, it was hard to distinguish the effects of pressure and Ca^{2+} concentration on the distribution and depth of protein bands. Only on a time scale, it could be seen that all protein bands became shallower from 5 to 120 min during intestinal digestion.

In the gastrointestinal tract, the degree of protein hydrolysis reflected the destruction of casein wall materials. Before digestion, HHP first dissociated and then recombined casein micelles. During recombination, the binding between micelle fragments was random. Therefore, there would be many aggregates of different sizes, as shown by the protein band at 70 kDa. In the stomach, the κ-casein on the surface of micelles would be quickly cut by pepsin, leading to the emergence of *para*-κ-casein and the formation of curds. And it was obvious that the degree of protein hydrolysis was largely affected by the coagulation degree. In the stomach, higher pressure and Ca^{2+} concentration helped to form more and harder curds, which provided a stronger barrier to inhibit protein hydrolysis. Therefore, these HHP-induced aggregates and individual casein components hydrolyzed more slowly and had a longer retention time in the stomach. But as digestion progressed, these large curds would still be constantly destroyed and individual proteins would

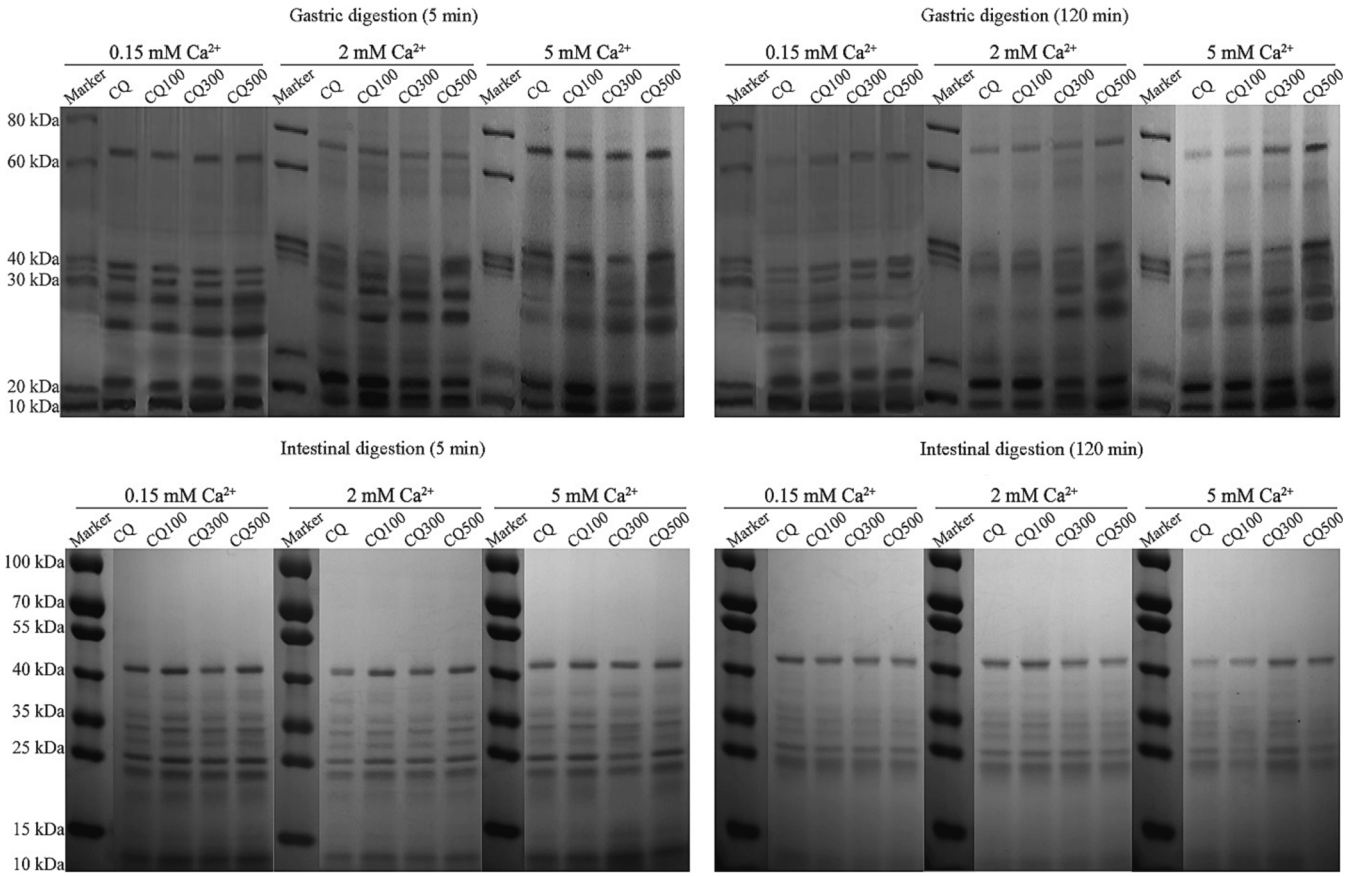

Fig. 5. The proteolysis results of quercetin-loaded casein delivery systems during *in vitro* digestion.

also be cleaved. Accordingly, some breakdown products would be observed in gastric juice. In the small intestine, these curds had a limited duration and were broken to dispersed small particles. The latter had a larger contact area and was easier to hydrolyze. Therefore, only some peptide fragments could be detected at this stage. If linked to the quercetin release results in Section 3.4, it could be said that the synergistic effect of higher pressure and Ca^{2+} helped to delay proteolysis by increasing the coagulation degree. More importantly, the slower proteolysis rate could maintain the integrity of the delivery systems and effectively inhibited the release of quercetin. In the intestinal environment, this inhibit effect could only be sustained to a certain extent under high pressure and Ca^{2+} concentration, but its ability was limited.

3.8. The mechanism summary

In this study, the research mechanism diagram was drawn in Fig. 6. Before digestion, HHP could open and reconstruct the micellar structure of casein. These recombinant casein micelles had smaller particle size and higher surface hydrophobicity, showing higher quercetin loading capacity. During *in vitro* digestion, the digestion behaviors of the delivery system were dominated by the micellar casein wall material. In the stomach, the contribution of κ-casein to the stability of the entire micelle system would be weakened by gastric acid and pepsin, leading to further aggregation. On the other hand, more α- and β-casein molecules originally existed in the micelles before digestion were exposed under higher pressure. These exposed α- and β-casein had ability to bind the free Ca^{2+} and further resulted in the CCP calcium bridge cross-linking between neighboring particles to form curds. Moreover, it was very important that the introduction of more exogenous calcium during digestion would also increase the number of cross-linked CCP calcium bridges. Therefore, micellar casein was more likely to interact with each other and formed more tightly structured curds under the synergistic effect of higher pressure and more Ca^{2+}, further reducing protein hydrolysis and quercetin release. In the intestinal tract, alkaline pH and Pancreatin no more supported the stabilization of these curds and further improved the protein hydrolysis degree. By contrast, these larger curds formed under higher pressure and Ca^{2+} concentration disintegrated more slowly. Consequently, the controlled release ability of these samples lasted longer and the degradation degree of quercetin was lower.

4. Conclusion

In this study, the micellar structure of casein was modified by HHP and then quercetin-loaded casein delivery systems were prepared. With the aim of exploring the effects of exogenous calcium incorporation in complex food matrices, calcium chloride was added to investigate the gastrointestinal digestion behaviors of delivery systems. The basic physicochemical results indicated that recombinant casein micelles have higher loading capacity for quercetin and improved the stability of the delivery systems. And the interaction results indicated that hydrogen bonds and hydrophobic interactions supported the formation of the delivery systems. During *in vitro* digestion, the digestion behaviors of recombinant casein micelles dominated the release of quercetin in the whole delivery systems. In the stomach, higher pressure and Ca^{2+} concentration aggravated the coagulation of casein and reduced the degree of protein hydrolysis, which further inhibited the release of quercetin. In the small intestine stage, although it appeared that the decomposition rate of curd was slower under higher pressure and Ca^{2+} concentration, the protein hydrolysis degree and quercetin release content were still significantly improved. Based on the structure and digestion behaviors of casein micelles, the results in this study indicated that the controlled release of active substances in casein-based delivery systems could be achieved through the application of environmental-friendly physical processing technology. And when developing functional foods such as high calcium foods, it is necessary to carefully consider the impact of exogenous calcium addition on the digestion and absorption of other nutrients.

CRediT authorship contribution statement

Minjie Liao: Conceptualization, Investigation, Methodology, Writing – original draft. **Wei Li:** Conceptualization, Data curation, Methodology, Writing – original draft. **Lu Peng:** Conceptualization, Investigation, Methodology. **Jiahao Li:** Conceptualization, Investigation. **Jinbo Ren:** Conceptualization, Investigation. **Kaixin Li:** Conceptualization, Methodology. **Fang Chen:** Data curation, Methodology. **Xiaosong Hu:** Methodology, Supervision. **Xiaojun Liao:** Data curation, Formal analysis. **Lingjun Ma:** Conceptualization, Supervision, Visualization. **Junfu Ji:** Conceptualization, Supervision, Writing – review & editing.

Declaration of competing interest

The authors declare that they have no known competing financial interests or personal relationships that could have appeared to influence the work reported in this paper.

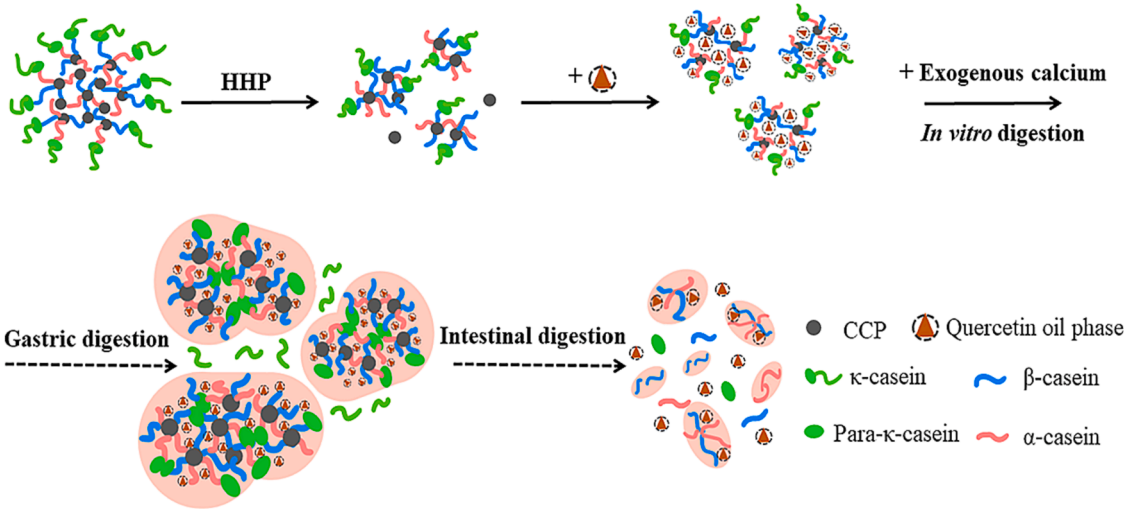

Fig. 6. The preparation and release mechanism of quercetin-loaded casein delivery systems.

Data availability

The data that has been used is confidential.

Acknowledgments

The study was supported financially by National Key R&D Program of China (Grant no. 2023YFF1104003) and National Natural Science Foundation of China (Grant no. 32372360 & 32101983).

References

Boland, M. J., Golding, M., & Singh, H. (2014). *Food Structures, Digestion and Health.*

Bourassa, P., Bariyanga, J., & Tajmir-Riahi, H. A. (2013). Binding sites of resveratrol, genistein, and curcumin with milk α- and β-caseins. *The Journal of Physical Chemistry B, 117*(5), 1287–1295.

Brodkorb, A., Egger, L., Alminger, M., Alvito, P., Assuncao, R., Ballance, S., Bohn, T., Bourlieu-Lacanal, C., Boutrou, R., Carriere, F., Clemente, A., Corredig, M., Dupont, D., Dufour, C., Edwards, C., Golding, M., Karakaya, S., Kirkhus, B., Le Feunteun, S., Lesmes, U., Macierzanka, A., Mackie, A. R., Martins, C., Marze, S., McClements, D. J., Menard, O., Minekus, M., Portmann, R., Santos, C. N., Souchon, I., Singh, R. P., Vegarud, G. E., Wickham, M. S. J., Weitschies, W., & Recio, I. (2019). INFOGEST static in vitro simulation of gastrointestinal food digestion. *Nature Protocols, 14*(4), 991–1014.

Broyard, C., & Gaucheron, F. (2015). Modifications of structures and functions of caseins: A scientific and technological challenge. *Dairy Science & Technology, 95*(6), 831–862.

Cepero-Betancourt, Y., Opazo-Navarrete, M., Janssen, A. E. M., Tabilo-Munizaga, G., & Pérez-Won, M. (2020). Effects of high hydrostatic pressure (HHP) on protein structure and digestibility of red abalone (Haliotis rufescens) muscle. *Innovative Food Science and Emerging Technologies, 60*, Article 102282.

De kruif, C. G. (1999). Casein micelle interactions. *International Dairy Journal, 9*(3–6), 183–188.

Do, A. B., Williams, K., & Toomer, O. T. (2016). In vitro digestibility and immunoreactivity of bovine milk proteins. *Food Chemistry, 190*(1), 581–587.

Du, Z., Xu, N., Yang, Y., Li, G., Tai, Z., Li, N., & Sun, Y. (2023). Study on internal structure of casein micelles in reconstituted skim milk powder. *International Journal of Biological Macromolecules, 224*, 437–452.

Elzoghby, A. O., Helmy, M. W., Samy, W. M., & Elgindy, N. A. (2013). Spray-dried casein-based micelles as a vehicle for solubilization and controlled delivery of flutamide: Formulation, characterization, and in vivo pharmacokinetics. *European Journal of Pharmaceutics & Biopharmaceutics, 84*(3), 487–496.

Fanny, L., Arnaud, S.-J., Frédéric, V., Christelle, L., Mireille, G.-D., Marie-Noëlle, M., Eric, B., & Frédéric, G. (2017). Gradual disaggregation of the casein micelle improves its emulsifying capacity and decreases the stability of dairy emulsions. *Food Hydrocolloids, 63*, 189–200.

Farrell, H. M., Jimenez-Flores, R., Bleck, G. T., Brown, E. M., Butler, J. E., Creamer, L. K., Hicks, C. L., Hollar, C. M., Ng-Kwai-Hang, K. F., & Swaisgood, H. E. (2004). Nomenclature of the Proteins of Cows'. *Milk—Sixth Revision, 87*(6).

Ghasemi, S., & Abbasi, S. (2014). Formation of natural casein micelle nanocapsule by means of pH changes and ultrasound. *Food Hydrocolloids, 42*(1), 42–47.

Han, T., Wang, M., Wang, Y., & Tang, L. (2020). Effects of high-pressure homogenization and ultrasonic treatment on the structure and characteristics of casein. *LWT-Food Science and Technology, 130*, 0023–6438.

Hudson, E. A., Rezende, J.d. P., Campos de Paula, H. M., Coelho, Y. L., Mendes da Silva, L. H., & dos Santos Pires, A. C. (2019). Energetic parameters of beta-casein/quercetin activated and thermodynamically stable complex formation accessed by Surface Plasmon Resonance. *Colloids and Surfaces B: Biointerfaces, 181*(1), 798–805.

Huppertz, T., & Chia, L. W. (2021). Milk protein coagulation under gastric conditions: A review. *International Dairy Journal, 113*, 0958–6946.

Huppertz, T., Heck, J., Bijl, E., Poulsen, N. A., & Larsen, L. B. (2021). Variation in casein distribution and mineralisation in the milk from Holstein-Friesian cows. *International Dairy Journal, 119*, 0958–6946.

Huppertz, T., & Lambers, T. T. (2020). Influence of micellar calcium phosphate on in vitro gastric coagulation and digestion of milk proteins in infant formula model systems. *International Dairy Journal, 107*, Article 104717.

Iturmendi, N., García, A., Galarza, U., Barba, C., Fernández, T., & Maté, J. I. (2020). Influence of high hydrostatic pressure treatments on the physicochemical, microbiological and rheological properties of reconstituted micellar casein concentrates. *Food Hydrocolloids, 106*(S1), Article 105880.

Ke, C., Liu, B., Dudu, O. E., Zhang, S., Meng, L., Wang, Y., Wei, W., Cheng, J., & Yan, T. (2023). Modification of structural and functional characteristics of casein treated with quercetin via two interaction modes: Covalent and non-covalent interactions. *Food Hydrocolloids, 137*, Article 108394.

Li, H., Wang, D., Liu, C., Zhu, J., Fan, M., Sun, X., Wang, T., Xu, Y., & Cao, Y. (2019). Fabrication of stable zein nanoparticles coated with soluble soybean polysaccharide for encapsulation of quercetin. *Food Hydrocolloids, 87*(2), 342–351.

Li, L., Lei, X., Chen, L., Li, W., Ma, Y., Luo, J., Liu, X., Xu, X., Zhou, G., & Feng, X. (2023). Protective mechanism of quercetin compounds against acrylamide-induced hepatotoxicity. *Food Science and Human Wellness, 13*(1), 225–240.

Li, N., & Zhong, Q. (2020). Casein core-polysaccharide shell nanocomplexes stable at pH 4.5 enabled by chelating and complexation properties of dextran sulfate. *Food Hydrocolloids, 103*, 0268-0005X.

Liao, M., Ma, L., Miao, S., Hu, X., & Ji, J. (2021). The in-vitro digestion behaviors of milk proteins acting as wall materials in spray-dried microparticles: Effects on the release of loaded blueberry anthocyanins. *Food Hydrocolloids, 115*(1), 0268-0005X.

Little, E. M., & Holt, C. (2004). An equilibrium thermodynamic model of the sequestration of calcium phosphate by casein phosphopeptides. *European Biophysics Journal, 33*(5), 435–447.

Liu, W., Kong, Y., Ye, A., Shen, P., Dong, L., Xu, X. X., Hou, Y., Wang, Y., Jin, Y., & Han, J. (2020). Preparation, formation mechanism and in vitro dynamic digestion behavior of quercetin-loaded liposomes in hydrogels. *Food Hydrocolloids, 104*(0268–005X).

Mao, M., Ni, D., Ma, L., Chen, F., Hu, X., & Ji, J. (2022). Impact of high hydrostatic pressure on the micellar structures and physicochemical stability of casein nanoemulsion loading quercetin. *Food Chemistry: X, 14*, Article 100356.

Mcsweeney, P. L. H., & Fox, P. F. (2013). *Advanced dairy chemistry: Volume 1A: Proteins: Basic aspects*, 4th edition.

Meena, G. S., Singh, A. K., Arora, S., Borad, S., Sharma, R., & Gupta, V. K. (2017). Physico-chemical, functional and rheological properties of milk protein concentrate 60 as affected by disodium phosphate addition, diafiltration and homogenization. *Journal of Food Science & Technology, 54*(6), 1678–1688.

Menéndez-Aguirre, O., Kessler, A., Stuetz, W., Grune, T., Weiss, J., & Hinrichs, J. R. (2014). Increased loading of vitamin D2 in reassembled casein micelles with temperature-modulated high pressure treatment. *Food Research International, 64*, 74–80.

Nassar, K. S., Lu, J., Pang, X., Ragab, E. S., Yue, Y. Y., Obaroakpo, U. J., Gebreyowhans, S., Hussain, N., Yang, B., Zhang, S., & Lv, J. (2021). The functionality of micellar casein produced from retentate caprine milk treated by HP - ScienceDirect. *Journal of Food Engineering, 288*(1), 110144.110141–110144.110111.

Nguyen, T. T. P., Bhandari, B., Cichero, J., & Prakash, S. (2015). Gastrointestinal digestion of dairy and soy proteins in infant formulas: An in vitro study. *Food Research International, 76*(10), 348–358.

Sadiq, U., Gill, H., & Chandrapala, J. (2021). Casein micelles as an emerging delivery system for bioactive food components. *Foods, 10*(8), 1965.

Silva, N. N., Piot, M., De Carvalho, A. F., Violleau, F., Fameau, A. L., & Gaucheron, F. (2013). pH-induced demineralization of casein micelles modifies their physico-chemical and foaming properties. *Food Hydrocolloids, 32*(2), 322–330.

Tan, C., Xue, J., Lou, X., Abbas, S., Guan, Y., Feng, B., Zhang, X., & Xia, S. (2014). Liposomes as delivery systems for carotenoids: Comparative studies of loading ability, storage stability and in vitro release. *Food & Function, 5*(6), 1232–1240.

Trujillo, A. J., Guamis, B., & Carretero, C. (1998). Hydrolysis of bovine and caprine caseins by rennet and plasmin in model systems. *Journal of Agricultural and Food Chemistry, 46*(8), 3066–3072.

Wang, K., Liu, D., Tao, X., Zhang, J., Huppertz, T., Regenstein, J. M., Liu, X., & Zhou, P. (2023). Decalcification strongly affects in vitro gastrointestinal digestion of bovine casein micelles under infant, adult and elderly conditions. *Food Hydrocolloids, 139*, Article 108515.

Wang, X., Ye, A., Lin, Q., Han, J., & Singh, H. (2018). Gastric digestion of milk protein ingredients: Study using an in vitro dynamic model. *Journal of Dairy Science, 101*(8), 6842–6852.

Ye, A. (2021). Gastric colloidal behaviour of milk protein as a tool for manipulating nutrient digestion in dairy products and protein emulsions. *Food Hydrocolloids, 115*(6), 106599.106591-106599.106515.

Yin, W., Song, L., Huang, Y., Chen, F., Hu, X., Ma, L., & Ji, J. (2022). Glycated alpha-lactalbumin based micelles for quercetin delivery: Physicochemical stability and fate of simulated digestion. *Food Chemistry-X, 13*, Article 100257.

Zhang, J., Liu, D., Xie, Y., Yuan, J., Wang, K., Tao, X., Hemar, Y., Regenstein, J. M., Liu, X., & Zhou, P. (2023). Gastrointestinal digestibility of micellar casein dispersions: Effects of caprine vs bovine origin, and partial colloidal calcium depletion using in vitro digestion models for the adults and elderly. *Food Chemistry, 416*(1), Article 135865.